

# We are IntechOpen, the world's leading publisher of Open Access books Built by scientists, for scientists

6,900

Open access books available

185,000

International authors and editors

200M

Downloads

Our authors are among the

154

Countries delivered to

TOP 1%

most cited scientists

12.2%

Contributors from top 500 universities



WEB OF SCIENCE™

Selection of our books indexed in the Book Citation Index  
in Web of Science™ Core Collection (BKCI)

Interested in publishing with us?  
Contact [book.department@intechopen.com](mailto:book.department@intechopen.com)

Numbers displayed above are based on latest data collected.  
For more information visit [www.intechopen.com](http://www.intechopen.com)



# Modeling of the Two-Dimensional Thawing of Logs in an Air Environment

*Nencho Deliiski, Ladislav Dzurenda and Natalia Tumbarkova*

## Abstract

A two-dimensional mathematical model has been created, solved, and verified for the transient nonlinear heat conduction in logs during their thawing in an air environment. For the numerical solution of the model, an explicit form of the finite-difference method in the computing medium of Visual FORTRAN Professional has been used. The chapter presents solutions of the model and its validation towards own experimental studies. During the validation of the model, the inverse task of the heat transfer has been solved for the determination of the logs' heat transfer coefficients in radial and longitudinal directions. This task has been solved also in regard to the logs' surface temperature, which depends on the mentioned coefficients. The results from the experimental and simulative investigation of 2D nonstationary temperature distribution in the longitudinal section of poplar logs with a diameter of 0.24 m, length of 0.48 m, and an initial temperature of approximately  $-30^{\circ}\text{C}$  during their many hours thawing in an air environment at room temperature are presented, visualized, and analyzed.

**Keywords:** heat conduction, modeling, logs, thawing, heat transfer coefficients, surface temperature

## 1. Introduction

The duration and the energy consumption of the thermal treatment of frozen logs aimed at their thawing and plasticizing for the production of veneer in winter are very high [1–9]. For example, thawing and plasticizing of poplar and pine logs with an initial temperature of  $-10^{\circ}\text{C}$  and moisture content of  $0.6\text{ kg}\cdot\text{kg}^{-1}$  about  $53\text{ kWh}\cdot\text{m}^{-3}$  and  $64\text{ kWh}\cdot\text{m}^{-3}$  thermal energy, respectively, are needed [9].

In the specialized literature, there are few reports about the temperature fields subjected to thawing in agitated water or steam frozen logs [7–21], and there is very scarce information about research of the temperature distribution in frozen logs during their thawing in an air environment given by the authors only [22].

The computation of the temperature field in logs during their thawing in water or steam is carried out using mathematical models, which solve the so-called direct task of the heat transfer. This is the task when all variables in the model are known, and this allows computing the temperature field in the body [23, 24].

The computation of the temperature field in logs during their thawing in an air environment requires solving of the so-called inverse task of the heat transfer. This

is the task when the model of the studied object and the experimentally obtained temperature field in it are known, but one or more variables in the model need to be determined during the solving and validation of the model [24].

The results from investigations of the temperature change subjected to thawing frozen logs only at conductive boundary conditions (i.e., at prescribed surface temperature) have been reported [2, 7–21].

The modeling and the multiparameter study of the thawing process of logs in air environment is of considerable scientific and practical interest. For example, as a result of such a study, it is possible to determine the real initial temperature of logs depending on their dimensions, wood species, moisture content, and the temperature of the air near the logs during their many days staying in an open warehouse before the thermal treatment in the production of veneer. The information about the real value of that immeasurable parameter can be used for scientifically based computing of the optimal, energy saving regimes for thermal treatment of each specific batch of logs.

This chapter presents the creation, numerical solving and validation of a two-dimensional nonlinear mathematical model of the transient heat conduction in frozen logs during their thawing at convective boundary conditions in an air environment. A validation of the models towards own experimentally determined 2D temperature distribution in poplar logs with a diameter of 0.24 m, length of 0.48 m, initial temperature of approximately  $-30^{\circ}\text{C}$ , and moisture content above the hygroscopic range during their 70 h thawing at room temperature has been carried out.

During the validation of the model, the inverse task has been solved for the determination of the unknown logs' heat transfer coefficients in radial and longitudinal directions. This task has been solved also in regard to the logs' surface temperature, which depends on the mentioned coefficients.

## 2. Mechanism of 2D heat distribution in logs during thawing

### 2.1 Mathematical model of the 2D temperature distribution in frozen logs during their thawing in an air environment

In [8] the following common form of a model, which describes the 2D nonstationary temperature distribution subjected to thawing frozen logs in an air environment, has been suggested:

$$c_{we-1,2,3} \cdot \rho_w \frac{\partial T(r, z, \tau)}{\partial \tau} = \lambda_{wr} \left[ \frac{\partial^2 T(r, z, \tau)}{\partial r^2} + \frac{1}{r} \cdot \frac{\partial T(r, z, \tau)}{\partial r} \right] + \frac{\partial \lambda_{wr}}{\partial T} \left[ \frac{\partial T(r, z, \tau)}{\partial r} \right]^2 + \lambda_{wp} \frac{\partial^2 T(r, z, \tau)}{\partial z^2} + \frac{\partial \lambda_{wp}}{\partial T} \left[ \frac{\partial T(r, z, \tau)}{\partial z} \right]^2 \quad (1)$$

with an initial condition

$$T(r, z, 0) = T_{w0-avg} \quad (2)$$

and boundary conditions for convective heat transfer:

- Along the radial coordinate  $r$  on the logs' frontal surface during thawing

$$\frac{\partial T(r, 0, \tau)}{\partial r} = - \frac{\alpha_{wp}(r, 0, \tau)}{\lambda_{wp}(r, 0, \tau)} [T(r, 0, \tau) - T_m(\tau)] \quad (3)$$

- Along the longitudinal coordinate  $z$  on the logs' cylindrical surface during thawing

$$\frac{\partial T(0,z,\tau)}{\partial z} = -\frac{\alpha_{\text{wr}}(0,z,\tau)}{\lambda_{\text{wr}}(0,z,\tau)} [T(0,z,\tau) - T_m(\tau)] \tag{4}$$

In [8] solutions of Eq. (1) only at conductive boundary conditions for the case of autoclave steaming of logs aimed at their plasticizing in the production of veneer have been realized and graphically presented.

An approach for solving Eq. (1) at much more complicated convective boundary conditions and verification of model (1) to (4) is considered below.

2.2 Mathematical description of the thermophysical characteristics of logs

In **Figure 1** the three temperature ranges are presented, at which the process of the logs' thawing above the hygroscopic range is carried out, i.e., when  $u > u_{\text{fsp}}$ .

There thermophysical characteristics of the logs and of both the frozen and nonfrozen free and bound water in them during the separate temperature ranges are also shown. The information on these characteristics is very important for the solving of the model given above.

The mathematical descriptions of the thermal conductivities of nonfrozen wood,  $\lambda_{\text{w-nfr}}$ , and frozen wood,  $\lambda_{\text{w-fr}}$ , and also of the specific heat capacities of nonfrozen wood,  $c_{\text{w-nfr}}$ , frozen wood,  $c_{\text{w-fr}}$ , and frozen free and bound water in the wood,  $c_{\text{fw}}$  and  $c_{\text{bwm}}$ , have been suggested in [8, 9, 18] using the experimentally determined data in the dissertations by Kanter [25] and Chudinov [2] for their change as a function of  $t$  and  $u$ . According to the suggested in [8, 9, 18] approach, the wood thermal conductivity during thawing of logs with moisture content  $u$  above the hygroscopic range can be calculated with the help of the following equations for  $\lambda_{\text{w}}(T, u, \rho_{\text{b}}, u_{\text{fsp}})$ :

$$\lambda_{\text{w}} = \lambda_{\text{w0}} \cdot \gamma \cdot [1 + \beta \cdot (T - 273.15)], \tag{5}$$

$$\lambda_{\text{w0}} = K_{\text{ad}} \cdot v \cdot [0.165 + (1.39 + 3.8u) \cdot (3.3 \cdot 10^{-7} \rho_{\text{b}}^2 + 1.015 \cdot 10^{-3} \rho_{\text{b}})], \tag{6}$$

$$v = 0.1284 - 0.013u. \tag{7}$$

The coefficients  $\gamma$  and  $\beta$  in Eq. (5) are calculated using the next equations:

- For nonfrozen wood at  $u > u_{\text{fsp}}^{272.15}$  and  $272.15\text{K} < T \leq 423.15\text{K}$

$$\gamma = 1.0, \tag{8}$$

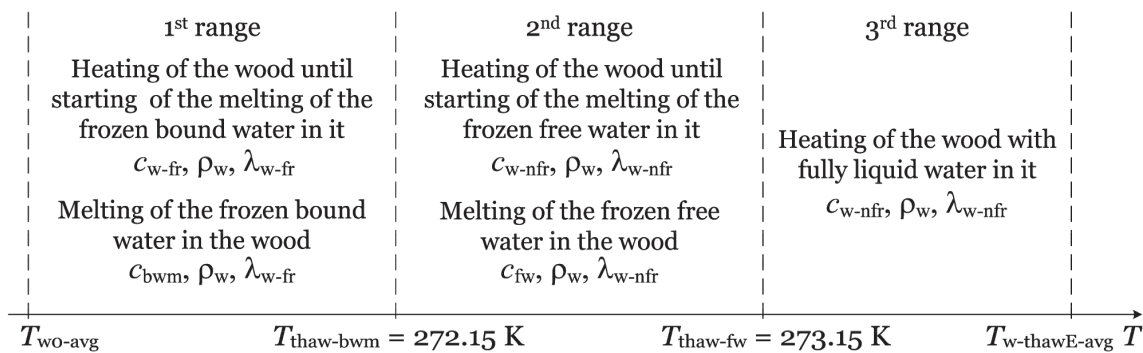


**Figure 1.** Temperature ranges of the logs' thawing process at  $u > u_{\text{fsp}}$  and thermophysical characteristics of the wood and of the frozen and nonfrozen bound and free water in it.

$$\beta = 3.65 \left( \frac{579}{\rho_b} - 0.124 \right) \cdot 10^{-3}. \quad (9)$$

- For frozen wood at  $u > u_{fsp}^{272.15}$  and  $213.15K \leq T \leq 272.15K$

$$\gamma = 1 + 0.34 [1.15(u - u_{fsp})], \quad (10)$$

$$\beta = 0.002(u - u_{fsp}) - 0.0038 \left( \frac{579}{\rho_b} - 0.124 \right). \quad (11)$$

The fiber saturation points of the wood species,  $u_{fsp}$  and  $u_{fsp}^{272.15}$ , are calculated according to following Eqs. [9]:

$$u_{fsp} = u_{fsp}^{293.15} - 0.001(T - 293.15), \quad (12)$$

and consequently

$$u_{fsp}^{272.15} = u_{fsp}^{293.15} + 0.021, \quad (13)$$

where  $u_{fsp}^{293.15}$  is the standardized fiber saturation point of the wood at  $T = 293.15$  K (i.e., at  $t = 20^\circ\text{C}$ ),  $\text{kg} \cdot \text{kg}^{-1}$ , and  $u_{fsp}^{272.15}$  is the fiber saturation point at  $T = 272.15$  K (i.e., at  $t = -1^\circ\text{C}$ ),  $\text{kg} \cdot \text{kg}^{-1}$ . At  $t = -1^\circ\text{C}$ , the melting of the frozen bound water in the wood is fully completed, and the melting of the free water in the wood starts [22, 26].

The effective specific heat capacities of the logs during the pointed three ranges of the thawing process,  $c_{we-1,2,3}$ , which participate in Eq. (1), are equal to the following:

$$\text{First range : } c_{we-1} = c_{w-fr} + c_{bwm}, \quad (14)$$

$$\text{Second range : } c_{we-2} = c_{w-nfr} + c_{fw}, \quad (15)$$

$$\text{Third range : } c_{we-3} = c_{w-nfr}. \quad (16)$$

According to the suggested in [8, 9, 22] mathematical description, the effective specific heat capacities of the logs during their thawing can be calculated with the help of the following equations for  $c_{we-1,2,3}(T, u, u_{fsp})$ :

$$c_{we-1,2,3} = \left\{ \begin{array}{l} \left[ 1.06 + 0.04u + \frac{0.00075(T - 272.15)}{u_{fsp}^{272.15}} \right] \cdot \frac{526 + 2.95T + 0.0022T^2 + 2261u + 1976u_{fsp}^{272.15}}{1 + u} + \\ + 1.8938 \cdot 10^4 \left( u_{fsp}^{272.15} - 0.12 \right) \cdot \frac{\exp[0.0567(T - 272.15)]}{1 + u} \\ @u > u_{fsp}^{272.15} \& 213.15K \leq T \leq 272.15K \quad (1^{st} \text{ range}) \\ \frac{2862u + 555}{1 + u} + \frac{5.42u + 2.95}{1 + u}T + \frac{0.0036}{1 + u}T^2 + \\ + 3.34 \cdot 10^5 \frac{u - u_{fsp}^{272.15}}{1 + u} \\ @u > u_{fsp}^{272.15} \& 272.15K < T < 273.15K \quad (2^{nd} \text{ range}) \\ \frac{2862u + 555}{1 + u} + \frac{5.42u + 2.95}{1 + u}T + \frac{0.0036}{1 + u}T^2 \\ @u > u_{fsp}^{272.15} \& 273.15K \leq T \leq 413.15K \quad (3^{rd} \text{ range}) \end{array} \right. \quad (17)$$

The wood density,  $\rho_w$ , which participates in Eq. (1), is determined above the hygroscopic range according to the following Equation [1–22, 27]:

$$\rho_w = \rho_b \cdot (1 + u). \quad (18)$$

### 2.3 Mathematical description of the heat transfer coefficients of logs

For solving of the 2D mathematical model given above, it is needed to have values for the heat transfer coefficients of the logs in radial and longitudinal directions,  $\alpha_{wr}$  and  $\alpha_{wp}$ , respectively, which participate in Eqs. (3) and (4).

As it was mentioned in the Introduction, the values of  $\alpha_{wr}$  and  $\alpha_{wp}$  can be computed by solving the inverse task of the heat transfer between the logs and surrounding air environment.

The calculation of  $\alpha_{wr}$  and  $\alpha_{wp}$  can be carried out with the help of the following equations of the similarity theory, which are valid for the cases of heating of horizontally situated cylindrical bodies in conditions of free air convection [28]:

$$\alpha_{wr} = \frac{Nu_r \cdot \lambda_a}{L}, \quad (19)$$

$$\alpha_{wp} = \frac{Nu_p \cdot \lambda_a}{D}, \quad (20)$$

$$Nu_r = f \left[ (Gr_r \cdot Pr_a)^{0.25} \cdot \left( \frac{Pr_a}{Pr_s} \right)^{0.25} \right], \quad (21)$$

$$Nu_p = f \left[ (Gr_p \cdot Pr_a)^{0.25} \cdot \left( \frac{Pr_a}{Pr_s} \right)^{0.25} \right], \quad (22)$$

$$Gr_r = \frac{g \cdot \beta_a \cdot L^3}{w_a^2} \cdot [T_m(\tau) - T_s(\tau)], \quad (23)$$

$$Gr_p = \frac{g \cdot \beta_a \cdot D^3}{w_a^2} \cdot [T_m(\tau) - T_s(\tau)], \quad (24)$$

$$Pr_a = \frac{w_a(T_a)}{a_a(T_a)}, \quad (25)$$

$$Pr_s = \frac{w_a(T_s)}{a_a(T_s)}, \quad (26)$$

For the usage of Eqs. (19)–(26), it is needed to have a mathematical description of the thermophysical characteristics of the air,  $\lambda$ ,  $\beta$ ,  $w$ , and  $a$ , depending on  $T$  and  $\varphi$ . The temperature of the air near the logs subjected to thawing during our experiments described below changes in the range from 243.15 to 303.15 K (i.e., from  $-30^\circ\text{C}$  to  $30^\circ\text{C}$ ), and  $\varphi$  changes from 40–100% (see **Figures 2** and **3**).

For the calculation of  $\lambda_a$ ,  $\beta_a$ ,  $w_a$ , and  $a_a$ , the temperature of the air,  $T_a$ , must be used, but for the calculation of  $w_s$  and  $a_s$  in Eq. (26), the temperature of the surface of the logs,  $T_s$ , has to be used.

In the accessible specialized sources, we did not find suitable mathematical descriptions of  $\lambda$ ,  $\beta$ ,  $w$ , and  $a$  of the air, depending on  $T$  and  $\varphi$ , which could be applied for the precise determination of  $\alpha_{wr}$  and  $\alpha_{wp}$  according to Eqs. (19)–(26).

Our further study has shown that for solving the inverse task of the heat transfer between the logs and surrounding air, i.e., for the calculation of the heat transfer coefficients of the logs, which participate in the boundary conditions (3) and (4) of the model, the following equations are suitable [29]:



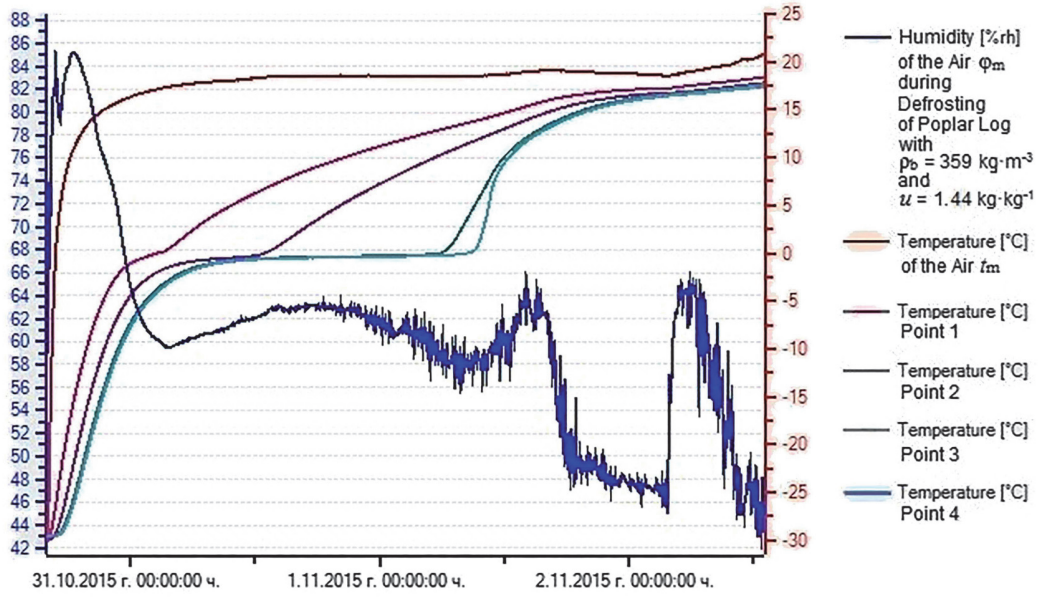


**Figure 2.**  
Experimentally determined change in  $t_m$ ,  $\varphi_m$ , and  $t$  in four points of the studied poplar log P1 during its 70 h thawing.

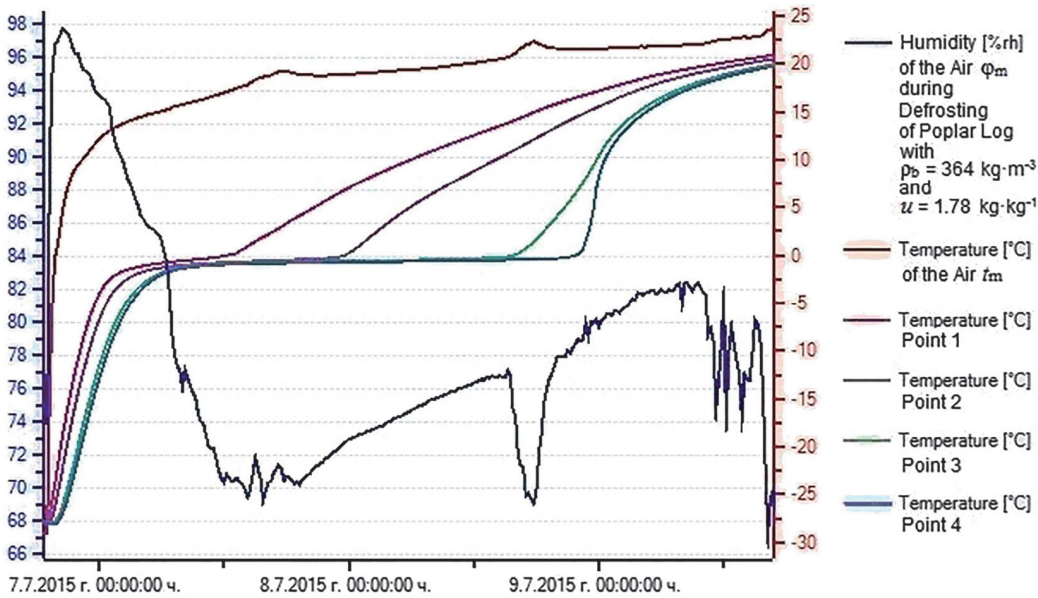


**Figure 3.**  
Experimentally determined change in  $t_m$ ,  $\varphi_m$ , and  $t$  in four points of the studied poplar log P2 during its 70 h thawing.

- In the radial direction on the cylindrical surface of the logs

$$\alpha_{wr} = 1.123[T(0, z, \tau) - T_m(\tau)]^x \quad (27)$$

- In the longitudinal direction on the frontal surface of the logs

$$\alpha_{wp} = 2.56[T(r, 0, \tau) - T_m(\tau)]^x \quad (28)$$

where  $x$  is an exponent, whose values are determined during the solving and validation of the model through the minimization of the root-square-mean error

(RSME) between the calculated model and experimentally obtained results about the change of the temperature fields subjected to thawing logs.

### 3. Experimental research of the thawing process of logs

#### 3.1 Experimental research of the 2D temperature distribution in poplar logs during their thawing

For solving the inverse task of the heat transfer aimed at validation of the suggested above mathematical model, it is necessary to have experimentally obtained data about the 2D temperature distribution in logs during their thawing. That is why we realized such experiments using poplar (*Populus nigra* L.) logs with  $D = 0.24$  m,  $L = 0.48$  m, and  $u > u_{fsp}$  [26].

In **Figure 4** the coordinates of four representative points of the logs, in which the 2D change in the temperature was measured and registered during the logs' thawing, are shown.

For the freezing of the logs before their thawing, a horizontal freezer was used with adjustable temperature range from  $-1$  to  $-30^{\circ}\text{C}$ . Sensors Pt100 with long metal casings were positioned in the drilled four holes of the logs. After 50 h separately freezing each logs, the freezer was switched off. Then its lid was opened, and 70 h thawing of the log at room temperature was carried out.

The automatic measurement and record of  $t_m$ ,  $\varphi_m$ , and  $t$  in the representative points of the logs during the experiments was accomplished by Data Logger type HygroLog NT3 produced by the Swiss firm ROTRONIC AG.

In **Figures 2 and 3**, the change in the temperature of the processing air medium,  $t_m$ , and in its humidity,  $\varphi_m$ , and also in the temperature in four representative points of two poplar logs, named below as P1 and P2, respectively, during their separate 70 h thawing is presented.

All curves of the experimentally obtained data on these figures are drawn using the licensed software HW4 of the Data Logger. The left coordinate axis on the figures is graduated at % of  $\varphi_m$ , and the right one is graduated at  $^{\circ}\text{C}$  of  $t$ .

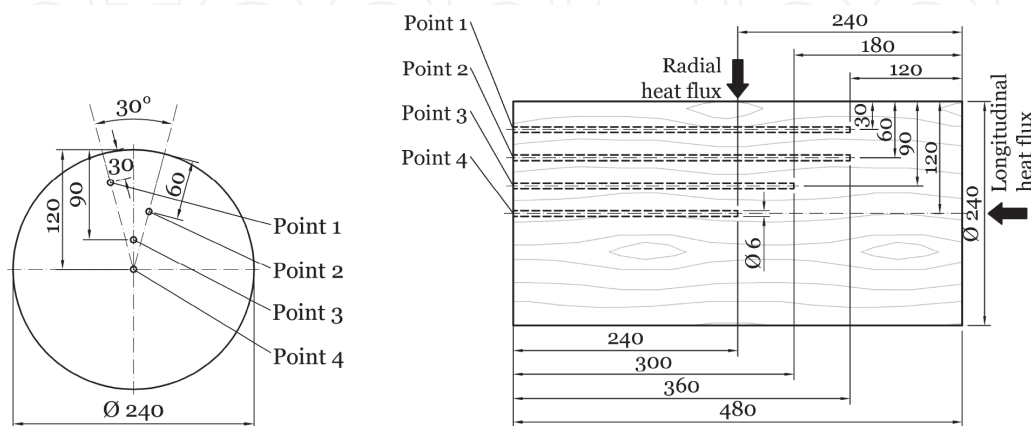


**Figure 4.** Radial (left) and longitudinal (right) coordinates of four characteristic points for the measurement of the temperature in logs subjected to thawing.



### 3.2 Mathematical description of the air medium temperature during logs' thawing

The change shown in **Figures 2 and 3** air medium temperature  $T_m$  during the logs' thawing with correlation 0.98 and root-square-mean error,  $\sigma < 1.5^\circ\text{C}$ , has been approximated with the help of the software package Table Curve 2D by the following equation:

$$T_m = \frac{a + c \cdot \tau^{0.5}}{1 + b \cdot \tau^{0.5}}, \quad (29)$$

whose coefficients are equal to:

- For log P1:  $a = 293.3637194$ ,  $b = -0.00236425$ ,  $c = -0.69281743$ .
- For log P2:  $a = 299.2738855$ ,  $b = -0.00245303$ ,  $c = -0.73047119$ .

and  $\tau$  is the sum of the time of logs' freezing, equal to 50 h = 180,000 s, and the current time of the subsequent thawing of the logs, s.

Eq. (29) was used for solving Eqs. (3) and (4) of the model.

## 4. Numerical solution of the mathematical model of the logs' thawing process

The mathematical descriptions of the thermophysical characteristics of the logs and also of  $T_m$  considered above were introduced in the mathematical model (1) to (4). An explicit form of the finite-difference method was used for solving of the model without any simplifications [7, 8].

### 4.1 Presentation of the model in a form suitable for programming

#### 4.1.1 Presentation of Eq. (1) of the model

The presentation of Eq. (1) of the model suitable for programming discrete analogue has been carried out using the given in **Figures 5 and 6** coordinate system.

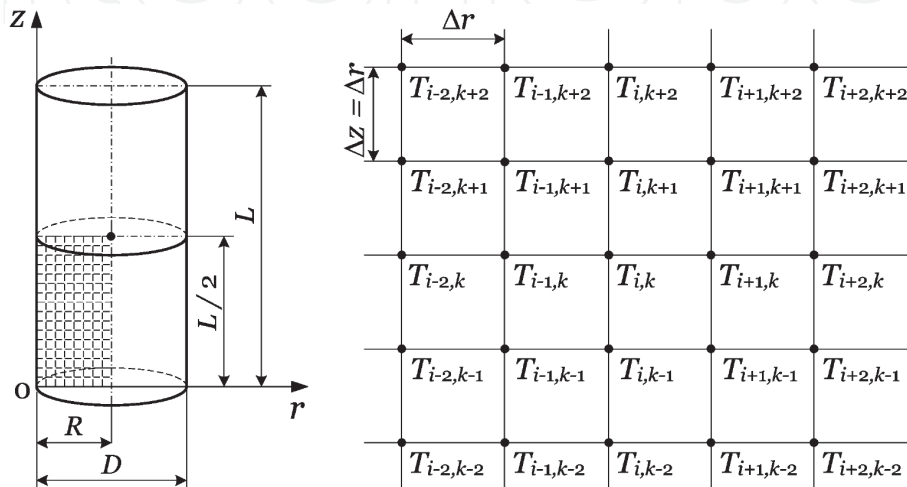


**Figure 5.** Positioning of the knots of 2D calculation mesh on  $1/4$  of longitudinal section of a log subjected to thawing (left) and calculation mesh for solving of the model (right).

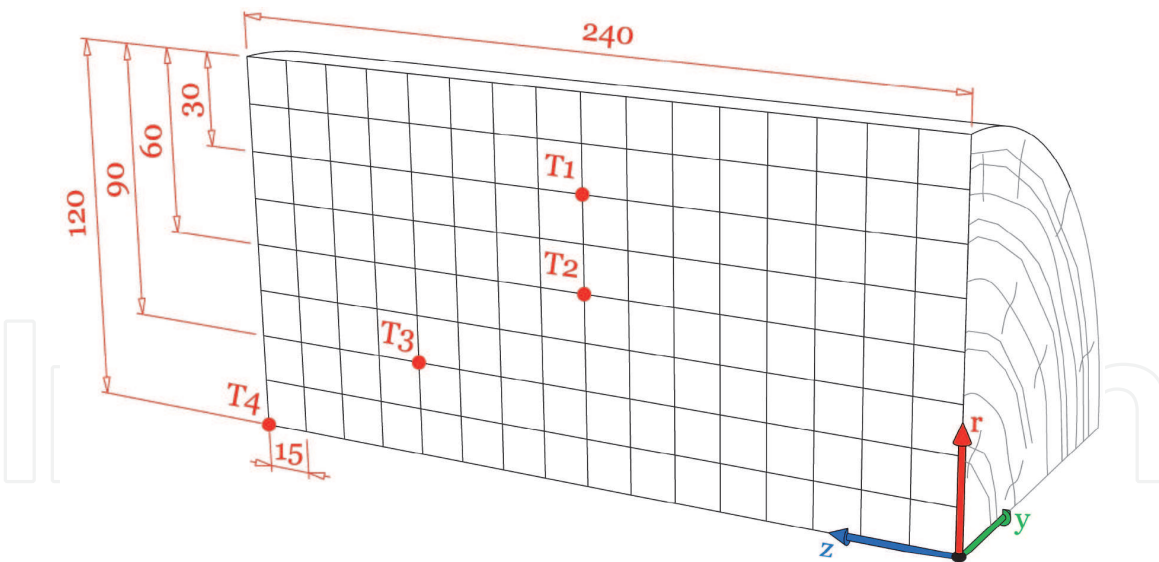


**Figure 6.**  
Calculation mesh and representative points  $T_1$ ,  $T_2$ ,  $T_3$ , and  $T_4$  on  $\frac{1}{4}$  of the longitudinal section subjected to thawing log.

These figures show the positioning of the knots of the calculation mesh and four representative points, in which the nonstationary 2D distribution of the temperature in the longitudinal section subjected to thawing log has been calculated. The mesh has been built on  $\frac{1}{4}$  of the longitudinal section of the log due to the fact that this  $\frac{1}{4}$  is mirrored symmetrical towards the remaining  $\frac{3}{4}$  of the same section.

Taking into consideration Eqs. (5) and (6), it can be written that

$$\lambda_w = \lambda_{w0r,p} \cdot \gamma \cdot [1 + \beta \cdot (T - 273.15)] \quad (30)$$

$$\lambda_{w0r} = K_{wr} \cdot v \cdot [0.165 + (1.39 + 3.8u) \cdot (3.3 \cdot 10^{-7} \rho_b^2 + 1.015 \cdot 10^{-3} \rho_b)] \quad (31)$$

$$\lambda_{w0p} = K_{wp} \cdot v \cdot [0.165 + (1.39 + 3.8u) \cdot (3.3 \cdot 10^{-7} \rho_b^2 + 1.015 \cdot 10^{-3} \rho_b)] \quad (32)$$

and using the coefficient

$$K_{wp/wr} = \frac{K_{wp}}{K_{wr}} \quad (33)$$

The discrete finite-difference analogue of the left-hand part of Eq. (1), which is suitable for programming in FORTRAN, has the following form [7, 30]:

$$c_{we-1,2,3} \cdot \rho_w \frac{\partial T(r, z, \tau)}{\partial \tau} \approx c_{we-1,2,3}^n \cdot \rho_w \frac{T_{i,k}^{n+1} - T_{i,k}^n}{\Delta \tau}. \quad (34)$$

Taking into account Eqs. (30), (31), and (32), the discrete analogue of the right-hand part of Eq. (1) has the following form:

$$\begin{aligned} & \lambda_{wr} \left[ \frac{\partial^2 T(r, z, \tau)}{\partial r^2} + \frac{1}{r} \cdot \frac{\partial T(r, z, \tau)}{\partial r} \right] + \frac{\partial \lambda_{wr}}{\partial T} \left[ \frac{\partial T(r, z, \tau)}{\partial r} \right]^2 + \\ & + \lambda_{wp} \frac{\partial^2 T(r, z, \tau)}{\partial z^2} + \frac{\partial \lambda_{wp}}{\partial T} \left[ \frac{\partial T(r, z, \tau)}{\partial z} \right]^2 = \{ \lambda_{w0r} \cdot \gamma \cdot [1 + \beta \cdot (T_{i,k}^n - 273.15)] \} \cdot \\ & \cdot \left[ \frac{T_{i-1,k}^n - 2T_{i,k}^n + T_{i+1,k}^n}{\Delta r^2} + \frac{1}{(i-1) \cdot \Delta r} \cdot \frac{T_{i-1,k}^n - T_{i,k}^n}{\Delta r} \right] + \beta \cdot \left( \frac{T_{i-1,k}^n - T_{i,k}^n}{\Delta r^2} \right)^2 + \\ & + \{ \lambda_{w0p} \cdot \gamma \cdot [1 + \beta \cdot (T_{i,k}^n - 273.15)] \} \cdot \frac{T_{i,k-1}^n - 2T_{i,k}^n + T_{i,k+1}^n}{\Delta z^2} + \beta \cdot \left( \frac{T_{i,k-1}^n - T_{i,k}^n}{\Delta z^2} \right)^2. \end{aligned} \quad (35)$$

After alignment of Eq. (34) with Eq. (35) and taking into account Eq. (33), at  $\Delta z = \Delta r$ , it is obtained that Eq. (1) is transformed into the following system of algebraic equations:

$$T_{i,k}^{n+1} = T_{i,k}^n + \frac{\lambda_{w0r} \cdot \gamma \cdot \Delta \tau}{c_{we-1,2,3}^n \cdot \rho_w \cdot \Delta r^2} \cdot \left\{ \begin{aligned} & \left[ 1 + \beta \cdot (T_{i,k}^n - 273.15) \right] \cdot \left[ T_{i-1,k}^n + T_{i+1,k}^n + K_{wp/wr} (T_{i,k-1}^n + T_{i,k+1}^n) - \right. \\ & \left. - (2 + 2K_{wp/wr}) T_{i,k}^n + \frac{1}{i-1} (T_{i-1,k}^n - T_{i,k}^n) \right] + \\ & \left. + \beta \cdot \left[ (T_{i-1,k}^n - T_{i,k}^n)^2 + K_{wp/wr} (T_{i,k-1}^n - T_{i,k}^n)^2 \right] \right\}. \end{aligned} \right. \quad (36)$$

The term  $\frac{1}{r}$  in the right-hand part of Eq. (1) is represented as  $\frac{1}{(i-1) \cdot \Delta r}$  in Eq. (35). According to the requirements of FORTRAN [7, 30], the knots of the calculation mesh, which are situated on the log's surfaces, are denoted by numbers  $i = 1$  and  $k = 1$  along the coordinate axes  $r$  and  $z$ , respectively.

The temperature in these surface knots is calculated with the help of Eqs. (38) and (42) given below. Since Eq. (36) calculates the temperature in the knots, which are located inside the logs, i.e., in the knots with  $i \geq 2$  and  $k \geq 2$ , the denominator of the term  $\frac{1}{i-1}$  in this equation is always greater than zero.

It can be noted that the effective specific heat capacities of the log during the pointed above three ranges of its thawing process (see **Figure 1**),  $c_{we-1}$ ,  $c_{we-2}$ , and  $c_{we-3}$ , which are unitedly represented as  $c_{we-1,2,3}$  in Eq. (36), are computed according to Eq. (17) separately for each knot of the calculation mesh.

#### 4.1.2 Presentation of the equation of the initial condition in the model

The initial condition (2) of the model of logs' thawing process obtains the following discrete finite-difference form:

$$T_{i,k}^0 = T_{w0-avg} \quad (37)$$

where  $T_{w0-avg}$  is the experimentally determined average mass temperature of the log at the beginning of the thawing process, K.

#### 4.1.3 Presentation of the equation of boundary condition in the model along the radial coordinate

The boundary condition (3) of the logs' thawing process obtains the following final form, suitable for programming in FORTRAN:

$$T_{i,1}^{n+1} = \frac{T_{i,2}^n + G_{i,1}^n \cdot T_m^{n+1}}{1 + G_{i,1}^n}. \quad (38)$$

The variable  $G_{i,1}^n$  in Eq. (38) is equal to

$$G_{i,1}^n = \frac{\Delta r \cdot \alpha_{wp}^n}{\lambda_{w0p} \cdot \gamma \cdot [1 + \beta \cdot (T_{i,1}^n - 273.15)]}, \quad (39)$$

where according to Eqs. (28) and (29)

$$\alpha_{wp}^n = 2.56 [T_{i,1}^n - T_m^n]^x, \quad (40)$$

where

$$T_m^n = \frac{a + c \cdot (n \cdot \Delta\tau)^{0.5}}{1 + b \cdot (n \cdot \Delta\tau)^{0.5}}. \quad (41)$$

#### 4.1.4. Presentation of the equation of boundary condition in the model along the longitudinal coordinate

Analogously, the boundary condition (4) of the logs' thawing process obtains the following final form, suitable for programming in FORTRAN:

$$T_{1,k}^{n+1} = \frac{T_{2,k}^n + G_{1,k}^n \cdot T_m^{n+1}}{1 + G_{1,k}^n}. \quad (42)$$

The variable  $G_{1,k}^n$  in Eq. (42) is equal to

$$G_{1,k}^n = \frac{\Delta r \cdot \alpha_{wr}^n}{\lambda_{w0r} \cdot \gamma \cdot [1 + \beta \cdot (T_{1,k}^n - 273.15)]}, \quad (43)$$

where according to Eq. (27)

$$\alpha_{wr}^n = 1.123 [T_{1,k}^n - T_m^n]^x \quad (44)$$

and  $T_m^n$  is calculated according to Eq. (41).

## 4.2 Input data for solving of the model

The numerical solving and verification of the model (1) to (4) has been realized in the calculation environment of Visual FORTRAN Professional.

Using own software package in that environment, computations were carried out for the determination of the 2D nonstationary change of  $t$  in the representative points of the logs P1 and P2, whose experimentally registered temperature fields are presented in **Figures 2** and **3**, respectively.

The initial temperature,  $t_{w0-avg}$ ; basic density,  $\rho_b$ ; and moisture content,  $u$ , of the logs during the experiments were as follows:

- For log P1:  $t_{w0-avg} = -29.7^\circ\text{C}$ ,  $\rho_b = 359 \text{ kg}\cdot\text{kg}^{-1}$ , and  $u = 1.44 \text{ kg}\cdot\text{kg}^{-1}$ .
- For log P2:  $t_{w0-avg} = -28.0^\circ\text{C}$ ,  $\rho_b = 364 \text{ kg}\cdot\text{kg}^{-1}$ , and  $u = 1.78 \text{ kg}\cdot\text{kg}^{-1}$ .

As it was mentioned above, the duration of the freezing and duration of the subsequent thawing of the logs were equal to 50 and 70 h, respectively.

The model was solved with step  $\Delta r = \Delta z = 0.006 \text{ m}$  along the coordinates  $r$  and  $z$ , with step  $\Delta\tau = 6 \text{ s}$  [8, 23], and with the same initial and boundary conditions, as they were during the experimental research.

During the solving of the model, mathematical descriptions of the thermophysical characteristics of poplar sapwood with  $u_{fsp}^{293.15} = 0.35 \text{ kg}\cdot\text{kg}^{-1}$ ,  $K_{wr} = 1.48$ , and  $K_{wp} = 2.88$  [7, 9] have been used.

### 4.3 Inverse determination of the heat transfer coefficients during solving of the model

The model (1) to (4) was solved with various values of the exponent  $x$  in Eqs. (27) and (28). The computed by the model change of  $t$  in the four representative points of the logs with each of the tested values of the exponent  $x$  during the thawing was compared mathematically with the corresponding one experimentally registered change of  $t$  in these points with an interval of 15 min.

The aim of this comparison was to determine the values of  $x$ , which ensure the best compliance between the computed and experimentally registered temperature fields in subjected to thawing logs.

As a criterion of the best compliance, the minimum average value of RSME,  $\sigma_{\text{avg}}$ , was used, which is equal to

$$\sigma_{\text{avg}} = \sqrt{\frac{\sum_{n=1}^N \sum_{p=1}^P (t_{p,n}^{\text{comp}} - t_{p,n}^{\text{exp}})^2}{P \cdot (N - 1)}}, \quad (45)$$

where  $t_{p,n}^{\text{comp}}$  and  $t_{p,n}^{\text{exp}}$  are the computed and experimentally registered temperatures in the representative points;  $p$  is the number of the representative points of the logs,  $p = 1, 2, 3, 4$ , i.e.,  $P = 4$  was inputted into Eq. (45);  $n$  is the number of the moments of the thawing process,  $(n = 1, 2, 3, \dots, N = \tau_{\text{thaw}})/(150\Delta\tau) = 252,000 \text{ s}/900 \text{ s} = 280$ , because of the circumstance that the comparison of the computed values of  $t$  with experimentally registered values in the same points was made with an interval of 15 min = 900 s = 150 $\Delta\tau$ .

For the calculation of  $\sigma_{\text{avg}}$ , a software program in the calculation environment of MS Excel was prepared. At  $\tau_{\text{thaw}} = 70 \text{ h} = 252,000 \text{ s}$ , RSME has been calculated with the help of the program simultaneously for a total of  $N \cdot P = 1120$  temperature–time points during the thawing of each log.

It was determined that the minimum values of RSME overall for the studied four representative points are equal to  $\sigma_{\text{avg}} = 1.37^\circ\text{C}$  for log P1 and to  $\sigma_{\text{avg}} = 1.34^\circ\text{C}$  for log P2. These minimum values of  $\sigma_{\text{avg}}$  correspond to the following values of the

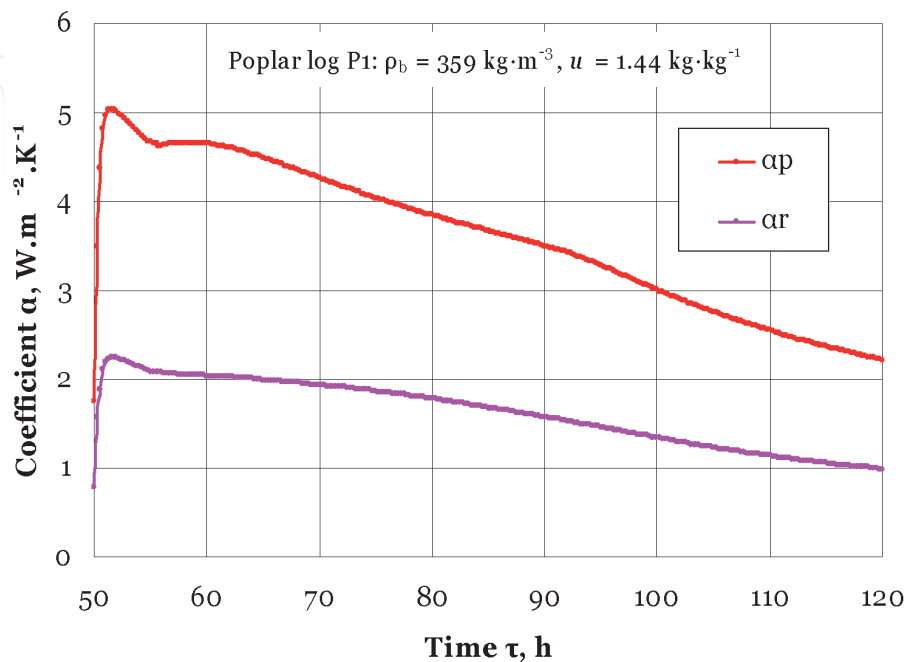


**Figure 7.**  
Calculated change in  $\alpha_{wv}$  and  $\alpha_{wp}$  of the log P1 during its 70 h thawing.



exponent  $x$  in Eqs. (27) and (28), which were obtained during the solving of the inverse task,  $x = 0.22$  for log P1 and  $x = 0.20$  for log P2.

**Figures 7 and 8** present the calculated change in  $\alpha_{wr}$  and  $\alpha_{wp}$  during the studied thawing process of the logs P1 and P2, respectively.

**Figures 9 and 10** present the calculated change in  $t_m$  and also in the logs' surface temperature  $t_s$  and  $t$  of 4 representative points of the studied logs.

It can be seen that with the decrease of the difference between  $t_m$  and  $t_s$  during the logs' thawing, the heat transfer coefficients on **Figures 7 and 8** gradually decrease, as follows:

- At  $\alpha_{wr}$ : from 2.3 to 1.0 W·m<sup>-2</sup>·K<sup>-1</sup> for P1 and from 1.9 to 1.2 W·m<sup>-2</sup>·K<sup>-1</sup> for P2.
- At  $\alpha_{wp}$ : from 5.1 to 2.2 W·m<sup>-2</sup>·K<sup>-1</sup> for P1 and from 4.5 to 2.8 W·m<sup>-2</sup>·K<sup>-1</sup> for P2.

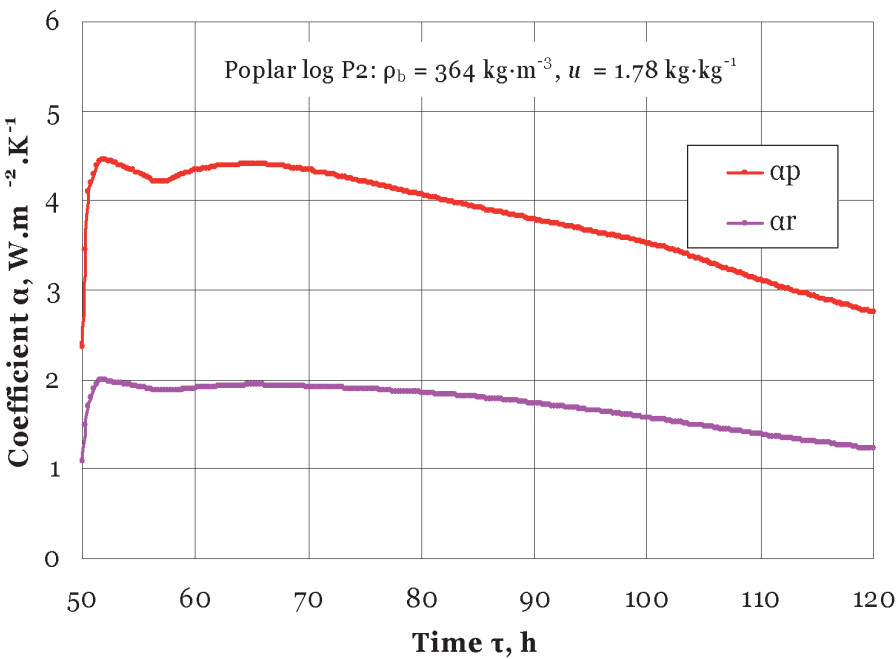


**Figure 8.**  
Calculated change in  $\alpha_{wr}$  and  $\alpha_{wp}$  of the log P2 during its 70 h thawing.

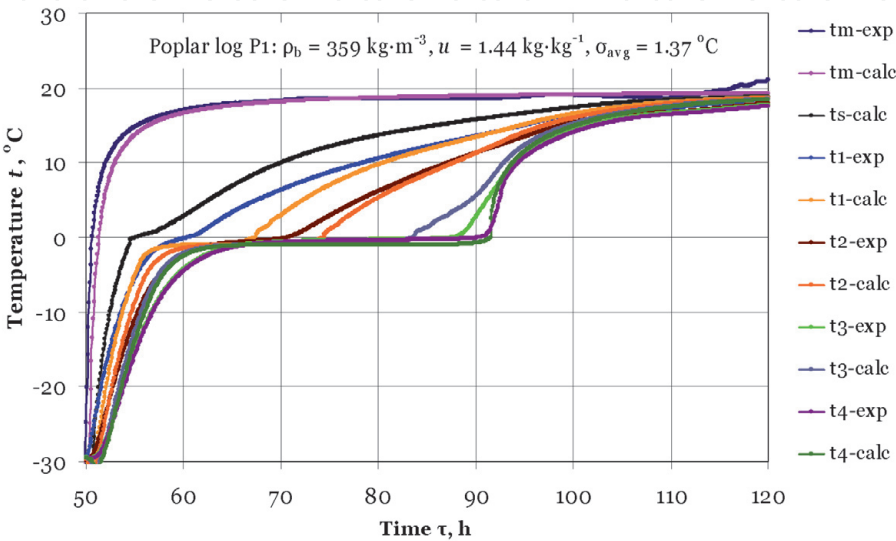


**Figure 9.**  
Experimentally determined and calculated change in  $t_m$ ,  $t_s$ , and  $t$  in four points of the log P1 during its 70 h thawing.

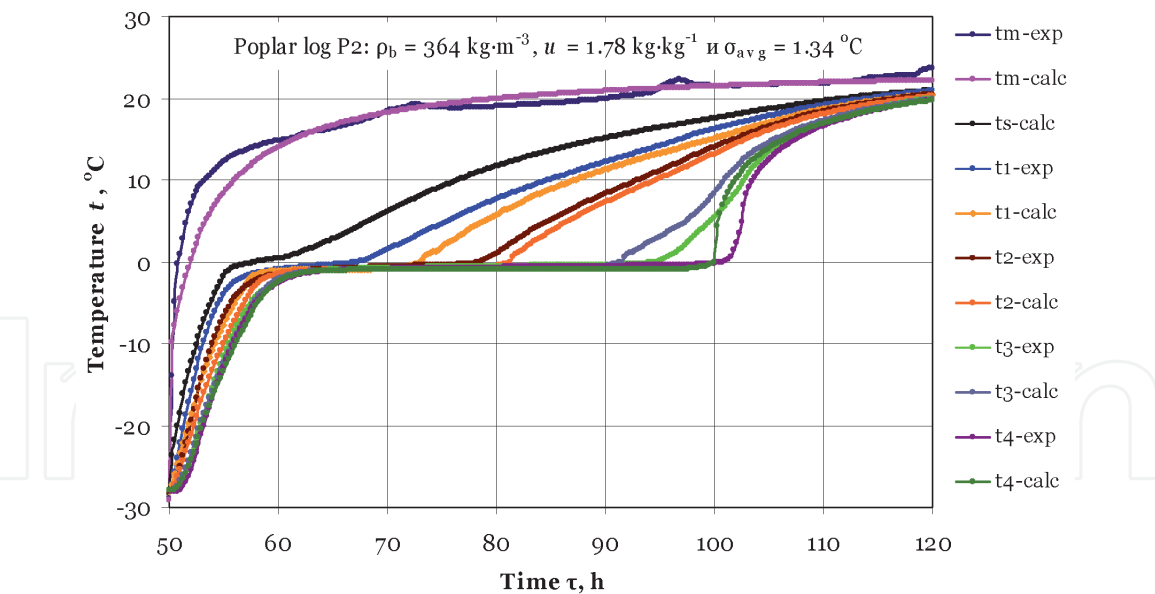


**Figure 10.** Experimentally determined and calculated change in  $t_m$ ,  $t_s$ , and  $t$  in four points of the log P2 during its 70 h thawing.

Using the obtained change in the heat transfer coefficients, the change in the logs' surface temperature during the thawing,  $t_s$ , has been calculated by the model (refer to **Figures 9** and **10**).

The comparison to each other of the analogical curves in **Figures 2** and **9**, and also in **Figures 3** and **10**, shows good conformity between the calculated and experimentally determined changes in the very complicated temperature fields of the studied logs during their thawing.

During our extensive simulations with the model (1) to (4), we established good qualitative and quantitative compliance between computed and experimentally determined temperature fields of logs from numerous wood species with different moisture content above the hygroscopic range [31].

The overall RSME for the studied four representative points in the logs does not exceed 5% of the temperature ranges between the minimal and maximal temperatures of each log during its thawing.

## 5. Conclusions

This chapter describes the creation, solving, and validation of a 2D nonlinear mathematical model for the transient heat conduction subjected to thawing frozen logs in an air environment.

The mechanism of the heat distribution in logs during their thawing has been described by a 2D equation of heat conduction at convective boundary conditions. For the numerical solving of the model with the help of explicit form of the finite-difference method, a software package has been prepared in the calculation medium of Visual FORTRAN Professional developed by Microsoft.

A validation of the model towards our own experimentally determined 2D temperature distribution in poplar logs with a diameter of 0.24 m, length of 0.48 m, and initial temperature about  $-30^{\circ}\text{C}$  during their 70 h separate thawing at room temperature has been carried out.

During the validation of the model, the inverse problem has been solved for the determination of the logs' heat transfer coefficients in radial and longitudinal

directions. This problem has been solved also in regard to the logs' surface temperature, which depends on the mentioned coefficients.

The following minimum values of the average RSME total for the temperature change in four representative points in each of the studied logs have been obtained:

- $\sigma_{\text{avg}} = 1.37^\circ\text{C}$  for log P1 with  $\rho_b = 359 \text{ kg}\cdot\text{m}^{-3}$  and  $u = 1.44 \text{ kg}\cdot\text{kg}^{-1}$ .
- $\sigma_{\text{avg}} = 1.34^\circ\text{C}$  for log P2 with  $\rho_b = 364 \text{ kg}\cdot\text{m}^{-3}$  and  $u = 1.78 \text{ kg}\cdot\text{kg}^{-1}$ .

During the solving of the inverse task, it was determined that the heat transfer coefficients subjected to thawing logs decrease gradually, as follows:

- At  $\alpha_{\text{wr}}$ : from 2.3 to 1.0  $\text{W}\cdot\text{m}^{-2}\cdot\text{K}^{-1}$  for P1 and from 1.9 to 1.2  $\text{W}\cdot\text{m}^{-2}\cdot\text{K}^{-1}$  for P2.
- At  $\alpha_{\text{wp}}$ : from 5.1 to 2.2  $\text{W}\cdot\text{m}^{-2}\cdot\text{K}^{-1}$  for P1 and from 4.5 to 2.8  $\text{W}\cdot\text{m}^{-2}\cdot\text{K}^{-1}$  for P2.

Good adequacy and precision of the model towards the results from extensive own experimental studies allow for the carrying out of various calculations with it, which are connected to the nonstationary temperature distribution in logs during their thawing in an air environment. For example, as a result of such calculations, it is possible to determine the real initial temperature of logs depending on their dimensions, wood species, moisture content, and the temperature of the air near the logs during their many days staying in an open warehouse before the thermal treatment in the production of veneer.

The information about the real value of that immeasurable parameter is needed for scientifically based computing of the optimal, energy saving regimes for thermal treatment of each specific batch of logs.

The model of the logs' thawing process can be applied also in the software for controllers used for advanced model predictive automatic control [20, 21, 32] of this treatment. The approach for solving of the inverse task of the heat transfer in this chapter could be further applied in the development and solving of analogous models, for example, for the calculation of the temperature fields during freezing or thawing processes of different wooden and other capillary porous materials.

## Acknowledgements

This document was supported by the APVV Grant Agency as part of the project, APVV-17-0456, as a result of work of authors and the considerable assistance of the APVV agency.

## Nomenclature

$a$	temperature conductivity, $\text{m}^2\cdot\text{s}^{-1}$
$c$	specific heat capacity, $\text{J}\cdot\text{kg}^{-1}\cdot\text{K}^{-1}$
$D$	diameter, m
$g$	acceleration of gravity, $g = 9.81 \text{ m}\cdot\text{s}^{-2}$
Gr	Grashoff's number of similarity
$L$	length, m
Nu	Nusselt's number of similarity
Pr	Prandtl's number of similarity
$R$	radius: $R = D/2$ , m

$r$	radial coordinate: $0 \leq r \leq R$ , m
$T$	temperature, K
$t$	temperature, °C
$u$	moisture content, $\text{kg} \cdot \text{kg}^{-1} = \%/100$
$w$	kinematic viscosity coefficient, $\text{m}^2 \cdot \text{s}^{-1}$
$x$	exponent, –
$z$	longitudinal coordinate: $0 \leq z \leq L/2$ , m
$\alpha$	heat transfer coefficients between log's surfaces and the surrounding air medium, $\text{W} \cdot \text{m}^{-2} \cdot \text{K}^{-1}$
$\beta$	coefficient of the volume expansion of the air, $\text{K}^{-1}$
$\lambda$	thermal conductivity (for wood or air), $\text{W} \cdot \text{m}^{-1} \cdot \text{K}^{-1}$
$\rho$	density, $\text{kg} \cdot \text{m}^{-3}$
$\sigma$	root-square-mean error (RSME), °C
$\tau$	time, s
$\varphi$	relative humidity, %
$\Delta r$	step along the coordinates $r$ and $z$ for solving of the model, m
$\Delta \tau$	step along the time coordinate for solving of the model, s

### Subscripts

a	air
avg	average (for mass temperature of logs or for root-square-mean error)
b	basic (for wood density, based on dry mass divided to green volume)
bw	bound water
bwm	maximum possible amount of the bound water in the wood
comp	computed
exp.	experimental
fr	freezing
fre	end of freezing
fsp	fiber saturation point
fw	free water
$i$	current number of the knot of the calculation mesh in the direction along the log's radius: $i = 1, 2, 3, \dots, 21 = (R/\Delta r + 1)$
$k$	current number of the knot of the calculation mesh in longitudinal direction of the logs: $k = 1, 2, 3, \dots, 41 = (L/2/\Delta r + 1)$
m	medium (for temperature of the air environment near the logs during their thawing process)
p	parallel to the wood fibers
r	radial direction
s	surface
thaw	thawing
w	wood
we	wood effective (for specific heat capacity)
w-fr	wood with frozen water in it
w-nfr	wood with fully liquid water in it
w0p	parallel to the wood fibers at °C
w0r	radial direction of wood at °C
0	initial or at 0°C
1,2,3	1 <sup>st</sup> , 2 <sup>nd</sup> , 3 <sup>rd</sup> (for temperature ranges of the logs' thawing process)
@	at
&	and simultaneously with this

**Superscripts**

$n$	current number of the step $\Delta\tau$ along the time coordinate during solving of the model: $n = 1, 2, 3, \dots, N = \tau_{\text{thaw}}/\Delta\tau$
272.15	at 272.15 K, i.e., at $-1^{\circ}\text{C}$
293.15	at 293.15 K, i.e., at $20^{\circ}\text{C}$

**Author details**

Nencho Deliiski<sup>1\*</sup>, Ladislav Dzurenda<sup>2</sup> and Natalia Tumbarkova<sup>1</sup>

1 University of Forestry, Sofia, Bulgaria

2 Technical University in Zvolen, Slovakia

\*Address all correspondence to: [deliiski@netbg.com](mailto:deliiski@netbg.com)

**IntechOpen**

© 2020 The Author(s). Licensee IntechOpen. This chapter is distributed under the terms of the Creative Commons Attribution License (<http://creativecommons.org/licenses/by/3.0>), which permits unrestricted use, distribution, and reproduction in any medium, provided the original work is properly cited. 



## References

- [1] Vorreiter L. Holztechnologisches Handbuch. Vien: Fromm; 1949. p. 2080
- [2] Chudinov BS. Theoretical research of thermo physical properties and thermal treatment of wood [thesis for DSc.]. Krasnojarsk, USSR: SibLTI; 1966 (in Russian)
- [3] Kollmann FF, Côté WA Jr. Principles of Wood Science and Technology. I. Solid Wood. Berlin, Heidelberg, New York: Springer-Verlag; 1984. p. 592
- [4] Shubin GS. Drying and Thermal Treatment of Wood. Moscow: Lesnaya Promyshlennost, USSR; 1990. p. e337 (in Russian)
- [5] Požgaj A, Chovanec D, Kurjatko S, Babiak M. Structure and Properties of Wood. 2nd ed. Bratislava: Priroda a.s; 1997. p. 485 (in Slovak)
- [6] Trebula P, Klement I. Drying and Hydro-Thermal Treatment of Wood. Slovakia: Technical University in Zvolen; 2002. p. 449 (in Slovak)
- [7] Deliiski N, Dzurenda L. Modelling of the Thermal Processes in the Technologies for Wood Thermal Treatment. Slovakia: Technical University in Zvolen; 2010. p. 224 (in Russian)
- [8] Deliiski N. Transient heat conduction in capillary porous bodies. In: Ahsan A, editor. Convection and Conduction Heat Transfer. Rijeka, Croatia: InTech Publishing House; 2011. pp. 149-176. DOI: 10.5772/21424
- [9] Deliiski N. Modelling of the Energy Needed for Heating of Capillary Porous Bodies in Frozen and Non-frozen States. Saarbrücken, Germany: Lambert Academic Publishing, Scholars' Press; 2013. p. 116. Available from: <http://www.scholars-press.com//system/covegenerator/build/1060>
- [10] Steinhagen HP. Computerized finite-difference method to calculate transient heat conduction with thawing. Wood and Fiber Science. 1986;**18**(3): 460-467
- [11] Steinhagen HP. Heat transfer computation for a long, frozen log heated in agitated water or steam – A practical recipe. Holz als Roh- und Werkstoff. 1991;**49**(7–8):287-290. DOI: 10.1007/BF02663790
- [12] Steinhagen HP, Lee HW, Loehnertz SP. LOGHEAT: A computer program of determining log heating times for frozen and non-frozen logs. Forest Products Journal. 1987;**37**(11/12): 60-64
- [13] Steinhagen HP, Lee HW. Enthalpy method to compute radial heating and thawing of logs. Wood and Fiber Science. 1988;**20**(4):415-421
- [14] Khattabi A, Steinhagen HP. Numerical solution to two-dimensional heating of logs. Holz als Roh- und Werkstoff. 1992;**50**(7–8):308-312. DOI: 10.1007/BF02615359
- [15] Khattabi A, Steinhagen HP. Analysis of transient non-linear heat conduction in wood using finite-difference solutions. Holz als Roh- und Werkstoff. 1993;**51**(4):272-278. DOI: 10.1007/BF02629373
- [16] Khattabi A, Steinhagen HP. Update of “numerical solution to two-dimensional heating of logs”. Holz als Roh- und Werkstoff. 1995;**53**(1):93-94. DOI: 10.1007/BF02716399
- [17] Deliiski N. Modelling and automatic control of heat energy consumption required for thermal treatment of logs. Drvna Industrija. 2004;**55**(4):181-199
- [18] Deliiski N. Computation of the wood thermal conductivity during

- defrosting of the wood. Wood Research. 2013;**58**(4):637-650
- [19] Deliiski N, Dzurenda L, Tumbarkova N, Angelski D. Computation of the temperature conductivity of frozen wood during its defrosting. Drvna Industrija. 2015; **66**(2):87-96. DOI: 10.5552/drind.2015.1351
- [20] Hadjiski M, Deliiski N. Cost oriented suboptimal control of the thermal treatment of wood materials. IFAC-Papers. 2015;**48**(24):54-59. DOI: 10.1016/j.ifacol.2015.12.056
- [21] Hadjiski M, Deliiski N. Advanced control of the wood thermal treatment processing. Cybernetics and Information Technologies, Bulgarian Academy of Sciences. 2016;**16**(2): 179-197. DOI: 10.1515/cait-2016-0029
- [22] Deliiski N, Tumbarkova N. Numerical solution to two-dimensional freezing and subsequent defrosting of logs. In: Iranzo A, editor. Heat and Mass Transfer—Advances in Science and Technology Applications. London: IntechOpen; 2015. p. 20. DOI: 10.5772/intechopen.84706
- [23] Whitaker S. Fundamental Principles of Heat Transfer. Oxford OX3 OBW: Pergamon Press; 1977. p. 574. eBook 9781483159430
- [24] Kozdoba LA. Methods for Solving of Non-linear Heat Transfer Tasks. Moscow: Nauka, USSR; 1975. p. 228 (in Russian)
- [25] Kanter KR. Investigation of the Thermal Properties of Wood [Thesis]. Moscow: MLTI, USSR; 1955 (in Russian)
- [26] Deliiski N, Tumbarkova N. A methodology for experimental research of the freezing process of logs. Acta Silvatica et Lignaria Hungarica. 2016; **12**(2):145-156. DOI: 10.1515/aslh-2016-0013
- [27] Hrčka R. Model in Free Water in Wood. Wood Research. 2017;**62**(6): 831-837
- [28] Marin E, Calderon A, Delgado-Vasallo O. Similarity theory and dimensionless numbers in heat transfer. European Journal of Physics. 2009;**30**: 439. DOI: 10.1088/0143-0807/30/3/001/meta
- [29] Telegin AS, Shvidkiy BS, Yaroshenko UG. Heat- and Mass Transfer. Moscow: Akademkniga; 2002. p. 456 (in Russian)
- [30] Dorn WS, McCracken DD. Numerical Methods with FORTRAN IV: Case Studies. New York: John Willej & Sons Inc.; 1972. p. 451
- [31] Tumbarkova N. Modelling of the freezing and thawing processes of logs and their energy consumption [PhD Thesis]. Bulgaria: University of Forestry in Sofia; 2019. p. 198 (in Bulgarian)
- [32] Hadjiski M, Deliiski N, Grancharova A. Spatiotemporal parameter estimation of thermal treatment process via initial condition reconstruction using neural networks. In: Hadjiski M, Atanasov KT, editors. Intuitionistic Fuzziness and Other Intelligent Theories and their Applications. Cham, Switzerland: Springer International Publishing AG; 2019. pp. 51-80. DOI: 10.1007/978-3-319-78931-6